JOURNAL OF OPTOELECTRONICS AND ADVANCED MATERIALS Vol. 10, No. 1, January 2008, p. 158 - 163

Synthesis and photoluminescence of perovskite-type Ca_2MgWO_6: Eu^{3+} micrometer phosphor

F. LEI, B. YAN*

Department of Chemistry, Tongji University, Siping Road 1239, Shanghai 200092, China

Red micrometer phosphor Ca_2MgWO_6: Eu^{3+} with double perovskite structure has been synthesized via conventional solid-state reaction of stoichiometric amounts of $CaCO_3$, WO_3, MgO and Eu_2O_3, which is characterized by powder X-ray diffraction (XRD), Scanning electron microscopy (SEM), UV-visible diffuse reflectance spectroscopy (UV-vis DRS), thermogravimetry - differential scanning calorimeter (TG-DSC) and Fourier transform infrared spectroscopy (FT-IR). At room temperature, the crystal structure of Ca_2MgWO_6: Eu^{3+} is orthorhombic, space group Pmm2, with lattice parameters a = 7.715 Å, b = 5.413 Å, c = 5.549 Å. The structure contains alternating MgO_6 and WO_6 octahedra. TG-DSC measurements as a functional of temperature indicate a structural transition and crystallization temperature. The TG-DSC curve is agree well with the theoretical value, the mass loss within the temperature ranging from 600 ~ 800 ℃ is associated with the decomposition of $CaCO_3$, and the crystallization temperature is at 1224 ℃. The UV-vis DRS shows that the absorption band in the 200 ~ 350 nm is the charge transfer transition of tungstate group. The photoluminescent spectrum (PL) and lifetime are discussed in details. The emission spectrum includes $^5D_0 \rightarrow {}^7F_J$ (J = 1, 2, 3 and 4) emissions appearing at 535, 613, 651 and 700 nm, respectively. The peak at 613 nm is dominant, since Eu^{3+} is at a site lack of inversion symmetry (S_4), the blue band emissions peaking at 465 and 487 nm were the charge transfer state of WO_6^{6-} group. Especially the lifetimes and quantum efficiency are estimated.

(Received December 1, 2007; accepted January 2008)

Keywords: Tungstate, Ca_2MgWO_6: Eu^{3+}, Double perovskite structure, $A_2B'B''O_6$, Photoluminescence

1. Introduction

The ideal perovskite ABO_3 is a corner-sharing cubic network of BO_6 octahedra with A cations occupying the 12 coordinate position between 8 BO_6 octahedra. If two atoms, B' and B", are placed on the B sublattice, a double perovskite is formed. Double perovskite (DP), a broad class of compounds, have been studied since 1960s [1]. In recent years, the structure of general formula $A_2B'B''O_6$ (A=Ca, Sr, Ba; B'=Mg, Ni, Fe, Co, Zn; B"=W, Mo) with double perovskite structure have attracted much attention for their structural diversity as well as important physical properties, like ferroelectric, dielectric, photophysical, photocatalytic and magnetoresistance properties [2-8]. The versatility of perovskites is due to their ability to adapt to unmatched A-O, B'-O-B" bond lengths in the $A_2B'B''O_6$ system as well as the formation of intergrowth structures and the ability to accommodate anion or cation vacancies [9]. Compounds of this type have the general formula $A_2B'B''O_6$, where the A ion is in 12 coordination, and B' and B" in 6 coordination. The B' and B" ions are ordered and both form an fcc lattice, their coordination octahedral share corners only [2]. The double perovskite structure can be represented as a three-dimensional network of alternating $B'O_6$ and $B''O_6$ octahedra. The diversity and importance of perovskites is largely due to their inherent stability yet flexibility in terms of doping with a variety of cations, therefore removing or injecting electrons into the electronic bands [10]. Over the preceding decade it has been established that the structure and magnetic properties of the ordered double perovskites can be systematically tuned by altering the number of d-electrons of the B-site cation or the size of the cations. These substitutions can result in significant structural distortions that can, in turn, have a critical influence on the optical properties of these compounds [11]. In view of the structural diversity and technologically important material properties exhibited by members of this family, the oxide Ca_2MgWO_6, a prototypical member of this family, is an ordered double perovskite of the $A_2B'B''O_6$ type with Mg and W atoms alternating on the B' and B" sites, respectively, has been known for some time, play an important role as ferroelectric and dielectric materials. S.J. Patwe et al had reported the thermal expansion behavior and crystal structure of Ca_2MgWO_6 by Rietveld refinement [4].

Luminescence of rare earth ions doped in perovskite compounds have become attractive during the past decade, not only for its use as a probe to investigating local centers of the crystal environment, but also in search of novel phosphors for display technologies [12-24]. Perovskite-type oxides phosphors have been found to be potential candidate in field emission display (FED) and

plasma display panel (PDP) devices because they are sufficiently conductive to release electric charges stored on the phosphor particle surfaces [12]. Though the family of double perovskite structural compounds has been investigated extensively as one kind of colossal magnetroresistance (CMR), till now, to the best of our knowledge, they haven't been investigated as one kind phosphor matrix. Especially little work has been performed on the preparation and photoluminescence properties of Eu-doped micro-sized Ca_2MgWO_6 phosphor. So a detailed study of crystal structure and their optical properties are needed for better understanding of these materials.

The aim of this article is to introduce one Ca_2MgWO_6: Eu^{3+} red phosphor which belong to the $A_2B'B''O_6$ (A = Ca, Sr, Ba; B' = Mg, Ni, Fe, Co, Zn, Mn; B'' = W, Mo) double perovskite series, and has been the subject of numerous studies because the compounds' interesting magnetic and structural properties [25]. Recently, we focus our attention on the photoluminescence properties of double perovskite-type compound Ca_2MgWO_6: Eu^{3+} which has been synthesized by conventional solid-state reaction. To better understand the photoluminescence properties, the crystal structure of Ca_2MgWO_6: Eu^{3+} was discussed in relation to the photoluminescence activities.

2. Experiments

Powder Ca_2MgWO_6:Eu^{3+} sample was synthesized by conventional solid-state reaction. All chemical reagents were of analytical grade and used as received without any purification. In a typical procedure, starting materials used were as follows: $CaCO_3$ (AR), MgO (AR), WO_3 (AR) and Eu_2O_3 (99.99 %). The mixed chemical powder in a stoichiometric ratio was initially ground in an agate mortar homogeneously for about 30 min, and then transferred into a corundum crucible and heated at 800 ℃, 900 ℃, 1100 ℃ and 1300 ℃ in air for 4 h, respectively.

The XRD patterns of the polycrystalline products were recorded in the 2θ range of 10–70° with step width of 0.02 ° and step time of 0.8 s, using Cu Kα radiation using an X-ray powder diffractometer (XRD, D/max, Rigaku, Tokyo, Japan) operating at 40 KV/60 mA.. The morphology and particle size of the as-prepared powders were characterized by scanning electron microscopy (SEM, JEOL, Model JEM-1230). Photoluminescence spectra were examined using a fluorescence spectrophotometer (SHIMADZU, RF-5301PC) with Xe lamp at room temperature. FT-IR data were collected with a Perkin–Elmer 2000 FT-IR spectrophotometer, and recorded in the 400–4000 cm^{-1} range using the KBr pellets (Vector 22-Bruker spectrometer). UV–visible diffuse reflectance spectrum (UV–vis DRS) of the samples were measured at room temperature with a UV-visible spectrophotometer (Shimadzu, UV-2550) using $BaSO_4$ as a reference. The TG-DSC examinations were performed with differential scanning calorimeter (Netzch DSC 404C) made by Netzch Co. A small piece of the powder weighing 10mg was used for the DSC measurement. The sample was kept in an Al_2O_3 crucible and another empty Al_2O_3 crucible was used for reference as they were heated together at a constant rate of 10 °C/min from 40 °C to 1300 °C. These measurements were carried out within the temperature range of 40-1300 ℃in air, using corundum crucibles and at the heating rate of 10K/min. Luminescent lifetimes of the sample were obtained with an Ediburg FLS 920 phosphorimeter using a 450 W xenon lamp as excitation source (pulse width, 3 μs).

3. Results and discussion

3.1 Characterization of basic properties

Fig. 1 shows a typical XRD pattern of the as-prepared products obtained at 1300 ℃ for 4 h, all the reflection peaks of the products can be easily indexed to the pure orthorhombic phase of Ca_2MgWO_6 with lattice parameters a = 7.715 Å, b=5.413 Å and c = 5.549 Å , which are in good agreement with the literature value (JCPDS card 48-0108). It is belong to Pmm2 [25] space group. These lattice parameters indicate the formation of an ordered lattice of the ideal perovskite. These unit cell parameters are related to the primitive ideal perovskite lattice as: $a_0 = b_0 \approx \sqrt{2} \times a_p$ and $c_0 \approx 2 \times a_p$, where a_p is ideal perovskite unit cell parameter [5]. It can be mentioned that possible impurity phase like $CaWO_4$ and $MgWO_4$ are not observed in the diffraction pattern at the given temperature, which indicate that the final sintering temperature has an important role in the formation of the phase pure compounds. The XRD pattern is different from the monoclinic structure S.J. Patwe had reported [4]. In most of the monoclinic double perovskite compounds, the monoclinic angle is very close to 90°, and thus it is a little difficult to differentiate the monoclinic and orthorhombic lattice [4].

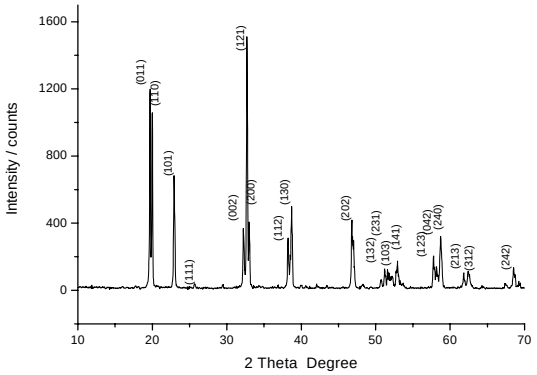

Fig. 1 XRD pattern of Ca_2MgWO_6: Eu^{3+} phosphor by solid-state reaction at 1300 ℃

Now we discuss the samples for which were sintered at different temperature were kinetically controlled. Fig.2.shows the XRD patterns of calcium magnesium tungstate synthesized by solid state reaction at different temperature of (a) 800 ℃, (b) 900 ℃, (c) 1100 ℃, (d) 1300 ℃ for 4 h. The phase purity of the product is ascertained by comparing the different calcination temperature. It can be mentioned here that the final sintering temperature has an important role in the formation of the phase pure compound. As can be seen from the XRD pattern of Fig.2 (a), the product was sintered at 800 ℃ for 4 h, with the same stoichiometric amount of raw materials, we just obtained the $CaWO_4$ and $MgWO_4$ phase. When sintered at 900 ℃, we obtained the $CaWO_4$ main phase, Fig. 2(c) shows the crystal phase obtained by sintered at 1100 ℃, we can obtain Ca_2MgWO_6 phase. Meanwhile, the $CaWO_4$ still exist as impurity phase. When we increase the temperature at 1300 ℃, Ca_2MgWO_6 can be obtained as the only one phase. So we can conclude that the optimal temperature for synthesize Ca_2MgWO_6 phase by solid-state reaction is at about 1300 ℃.

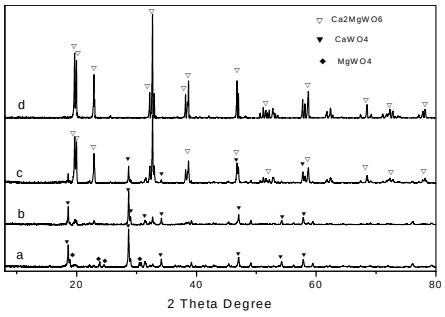

Fig. 2 XRD patterns of calcium magnesium tungstate by solid state reaction at different temperature with (a) 800 ℃, (b) 900 ℃, (c) 1100 ℃, (d) 1300 ℃.

The curve of thermogravimetry and differential scanning calorimetry (TG-DSC) are shown in Fig. 3 (a, b), the precursor was the mixture of $CaCO_3$, MgO, WO_3 and Eu_2O_3 as the starting materials, and their ratio is 1.96: 1: 1: 0.02. The temperature is range from 40 to 1300 ℃. In the TG curve, the obvious mass loss step, ranging from 600 ~ 900 ℃ can be associated with the process: $CaCO_3 \rightarrow CaO + CO_2\uparrow$, which is related to the decomposition of $CaCO_3$ and combination of W-O and Mg-O, the weight loss of CO_2 is 18.15 % (experimental value: 19 ~ 20 %; theoretical value: 18.15 %). From the DSC curve we can see an exothermic peak at around 724 ℃, accompanied by 18.15 % weight loss from 600 to 900 ℃, corresponding to the combination of MgO and WO_3, which is also agree well with the XRD pattern of the products sintered at 800 ℃. The endothermic peaking at about 1224 ℃ is related to the crystallization of Ca_2MgWO_6: Eu^{3+} and there is no obvious mass loss in the TG curve, it is in good agreement with the XRD pattern at 1300 ℃. The possible reaction process is as following:

$$2CaCO_3 \rightarrow 2CaO + 2CO_2\uparrow \quad (1)$$

$$MgO + WO_3 \rightarrow MgWO_4 \quad (2)$$

$$MgWO_4 + 2CaO \rightarrow Ca_2MgWO_6 \quad (3)$$

$$2CaCO_3 + MgO + WO_3 \rightarrow Ca_2MgWO_6 + 2CO_2\uparrow$$

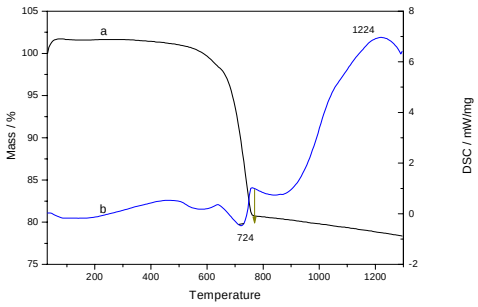

Fig. 3 TG-DSC curve of Ca_2MgWO_6: Eu^{3+} phosphor.

Fig. 4(a-d) shows the FT-IR spectra for the powders by solid state at different temperature (a) 800 ℃, (b) 900 ℃, (c) 1100 ℃, (d) 1300 ℃. The band at 3454 cm^{-1} is assigned to the O-H stretching mode of physically adsorbed water, which with the increase of reaction temperature became weaker. The band at 1635 cm^{-1} is the O-H bending mode. 800 cm^{-1} is WO_4^{2-}'s vibration. And at 807 cm^{-1} a strong band has appeared, it belongs to $CaWO_4$ [14]. As can be seen from Fig. 4(a) to (d), the peak at 807 cm^{-1} became weaker and till disappeared at Fig. 4(d). it is verified that with the temperature reached 1300 ℃, the $CaWO_4$ phase disappear. So it agreed well with the XRD patterns as above mentioned. The peak at 650 cm^{-1} is the vibration of WO_6^{6-} [15]. With the increase of the temperature, it became the main band of the IR spectrum.

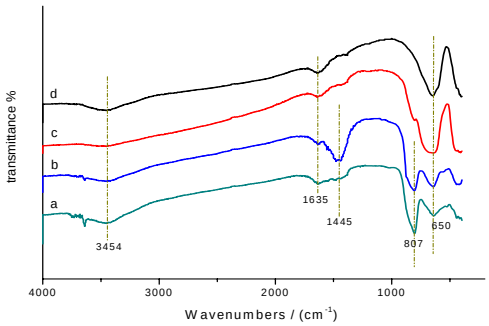

Fig. 4. FT-IR spectra of Ca_2MgWO_6: Eu^{3+} by solid-state reaction at different temperature: (a) 800 ℃, (b) 900 ℃, (c) 1100 ℃, (d) 1300 ℃

Typical SEM pictures of the samples the as-synthesized Ca_2MgWO_6 are shown in Fig. 5(A, B) It can be seen that both the product mainly consist of solid micron crystalline structures, which exist with some conglomeration among the crystalline grain for the high temperature 1100 ◦C of thermal decomposition. The typical crystalline grain is estimated to be around 1.0–2.0 μm in dimension. Besides this, the three-dimensional sizes of crystalline grain are very thick to afford high strengthen, it needs to refer that the crystalline powder and micrometer dimension for these powders with high strength would be very useful for the application to obtain high efficient phosphors because these micro crystalline materials can result in the high luminescent intensities [26].

3.2 Photoluminescent properties

To obtain information of the optical absorption of tungstate phosphor, diffuse reflectance spectra in the UV-vis region of Ca_2MgWO_6: Eu^{3+} samples synthesized at different temperature were recorded. These are shown in Fig. 6, the absorption band for all these samples was located within 200 to 350 nm, which is assigned to the absorption in the tungstate group corresponding to a so-called charge-transfer transition. The charge-transfer band depends strongly on the charge and radius of the cations surrounding the anion [16]. The luminescence intensity of 615 nm increases with the increasing of temperature, the maximum of the peak at 615 nm was shown in Fig. 4d, which was synthesized at 1300 ℃, it indicates that Eu^{3+} emission has high luminous efficiency in pure Ca_2MgWO_6 than in mixed compounds of $CaO{\cdot}MgO{\cdot}WO_3$. Ca_2MgWO_6 belongs to a promising material because of its broad band, it can be used as the matrix material.

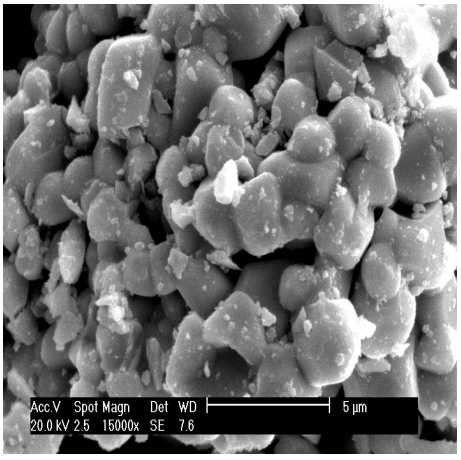

a

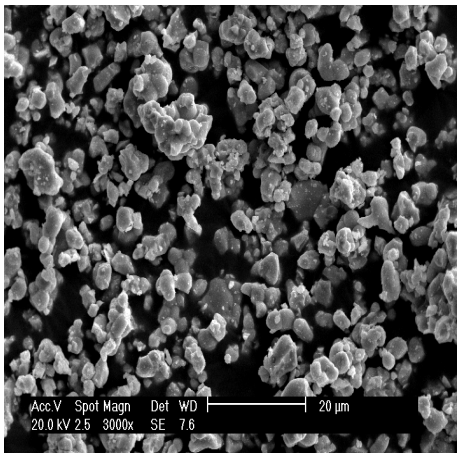

b

Fig. 5 SEM imagine of Ca_2MgWO_6: Eu^{3+} phosphor by solid-state reaction at 1300 ℃ a, b.

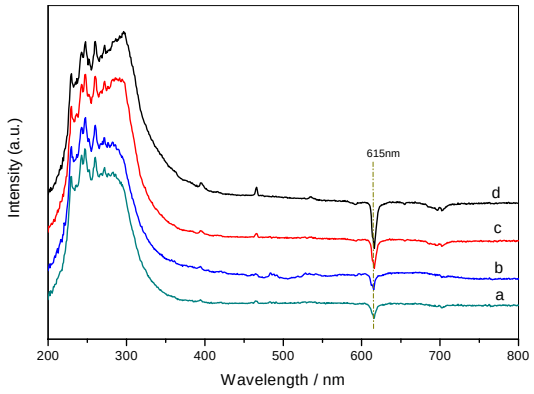

Fig. 6 UV-vis diffuse reflectance spectra of Ca_2MgWO_6: Eu^{3+} at different temperature: (a) 800 ℃; (b) 900 ℃; (c) 1100 ℃; (d) 1300 ℃

Fig.7. illustrates the excitation and emission spectra of Ca_2MgWO_6: Eu^{3+} phosphor synthesized at 1300 ℃. The excitation spectrum acquired by fixing the emission wavelength at 613 nm corresponding to the $^5D_0$-$^7F_2$ transition of Eu^{3+}, which shows a broad CTS (O→M (W and Eu)) band ranging from 350 to 450 nm along with sharp lines of Eu^{3+} ions at 360 nm, 380 nm, 393 nm, and 414 nm, corresponding the transition of $^7F_0$→$^5D_4$, $^7F_0$→$^5L_7$, $^7F_0$→$^5L_6$ and $^7F_0$→$^5D_2$, respectively. The majority of the emission spectrum of Ca_2MgWO_6: Eu^{3+}contains only the $^5D_0$-^7F_J transitions, indicating that the higher levels were coupled to tungstate stretching vibrations and quenched by cross-relaxation. The maximum excitation peak is at 393 nm. The emission spectrum was excited under 393 nm, which includes $^5D_0$→^7F_J (J = 1, 2, 3 and 4) emissions

appearing at 588, 613, 651 and 700 nm, respectively. It is well known that luminescence peaks of Eu^{3+} are sensitive to the symmetry around Eu^{3+} ions. The electric-dipole transition $^5D_0$-$^7F_2$ is only allowed when Eu^{3+} located at a site of non-inversion symmetry, while $^5D_0$-$^7F_1$ magnetic dipole transitions, at a site of inversion symmetry. Usually the luminescence intensity ratio of $^5D_0$-$^7F_2$ to $^5D_0$-$^7F_1$ is regarded as a probe to detect the inversion environmental symmetry around Eu^{3+} in the host. Based on the emission spectrum displayed in Fig. 7, the red $^5D_0$-$^7F_2$ transition (613 nm) dominates the spectrum and is definitely stronger than the orange $^5D_0$-$^7F_1$ transition (588 nm), and the ratio of $^5D_0$-$^7F_2$ to $^5D_0$-$^7F_1$ was calculated to be 5.6, the result indicates that the symmetry around Eu^{3+} is non-inversion. Since Eu^{3+} is at a site lack of inversion symmetry, the blue band emissions peaking at 465, 487 and 535 nm was the charge transfer state of WO_6^{6-}.

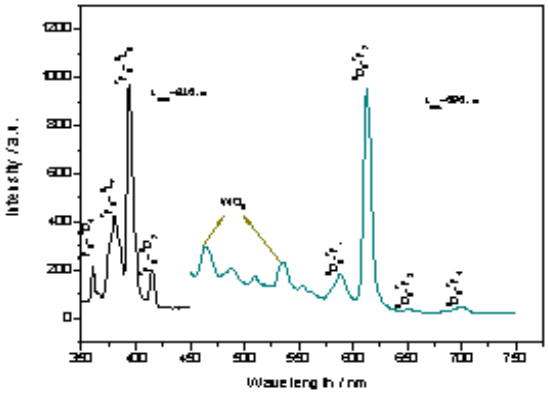

Fig. 7 PL spectrum of Ca_2MgWO_6: Eu^{3+} phosphor by solid-state reaction at 1300 ℃

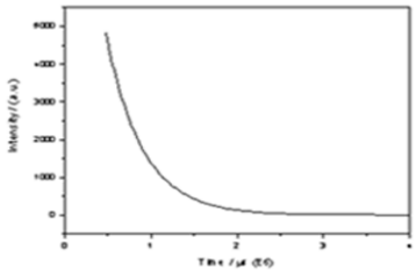

Fig. 8 Decay curve of Ca_2MgWO_6: Eu^{3+} phosphor by solid-state reaction at 1300 ℃.

The luminescence decay curves (Fig. 8) of the $^5D_0$ were obtained by monitoring the $^5D_0 \rightarrow {}^7F_2$ emission of Eu^{3+}. The typical decay curve of the Ca_2MgWO_6: Eu^{3+} were measured and they can be described as a single exponential ($Ln(S(t)/S_0) = -k_1t = -t/\tau$), indicating that all Eu^{3+} ions occupy the same average coordination environment. Furtherly, we selectively determined the emission quantum efficiencies of the $^5D_0$ europium ion excited state for Ca_2MgWO_6: Eu^{3+} on the basis of the emission spectra and lifetimes of the $^5D_0$ emitting level using the four main equations according to the ref. [27-34]. The detailed principle and method was adopted as ref. [35] and the data were shown in Table 1.

Table 1. Luminescent data for Ca_2MgWO_6: Eu^{3+}.

	Ca_2MgWO_6: Eu^{3+}			
Emission bands (nm)	588.4,	613.2,	651.4,	700.4
Energy levels (cm^{-1})	16995,	16308,	15352,	14278
experimental coefficients of spontaneous emissions (s^{-1})	50,	269.3,	6.9,	9.2
Lifetimes (ms) [b]	0.419			
Experimental decay rates (s^{-1})	2387			
Radiative decay rates (s^{-1})	335.4			
Non-radiative decay rates (s^{-1})	2051.6			
Quantum efficency (%)	14.05			

a: The Relative intensities were obtained by the calculation of integrated area of the corrected emission bands.

b: for $^5D_0 \rightarrow {}^7F_2$ transition of Eu^{3+}

$$A_{0J} = A_{01}\,(I_{0J} / I_{01})(\upsilon_{01} / \upsilon_{0J}) \quad (1)$$

$$A_{rad} = \Sigma A_{0J} = A_{01} + A_{02} + A_{03} + A_{04} \quad (2)$$

$$\tau = A_{rad}^{-1} + A_{nrad}^{-1} \quad (3)$$

$$\eta = A_{rad} / (A_{rad} + A_{nrad}) \quad (4)$$

Here A_{0J} is the experimental coefficients of spontaneous emissions, among A_{01} is the Einstein's coefficient of spontaneous emission between the $^5D_0$ and $^7F_1$ energy levels, which can be determined to be 50 s^{-1} approximately [32-34], and as a reference to calculate the value of other A_{0J}. I is the emission intensity and can be taken as the integrated intensity of the $^5D_0 \rightarrow {}^7F_J$ emission bands [27, 28]. υ_{0J} refers to the energy barrier and can be determined from the emission bands of Eu^{3+}'s $^5D_0 \rightarrow {}^7F_J$ emission transitions. A_{rad} and A_{nrad} mean to the radiative transition rate and nonradiative transition rate, respectively, among A_{rad} can be determined from the summation of A_{0J} (equation 2). And then the luminescence quantum efficiency can be calculated from the luminescent lifetimes, radiative and nonradiative transition rates. The luminescent quantum efficiency for Ca_2MgWO_6: Eu^{3+} is estimated to be 14.05 %, the deep luminescent behavior need to be study underway.

4. Conclusion

In conclusion, the uniform morphology micro-sized phosphor Ca_2MgWO_6: Eu^{3+}, with a double-perovskite crystal structure, was synthesized by the conventional

solid-state reaction method. It crystallizes in the orthorhombic space group with cell parameters a = 7.715 Å, b = 5.413Å, c = 5.549 Å (JCPDS 48-0108). The emission spectrum of Ca_2MgWO_6: Eu^{3+} includes $^5D_0$-^7F_J (J = 1, 2, 3 and 4) emissions appearing at 588, 613, 651 and 700 nm, respectively. Strong red emission from $^5D_0$-$^7F_2$ at 614 nm was observed in the Eu^{3+} doped Ca_2MgWO_6, since Eu^{3+} is at a site lack of inversion symmetry, the blue band emissions peaking at 465 and 487 nm were the charge transfer state of WO_6^{6-} group. The TG-DSC curve is agree well with the theoretical value, the mass loss within the temperature ranging from 600 ~ 800 ℃ is associated with the decomposition of $CaCO_3$, and the crystallization temperature is at 1224 ℃. The UV-vis DRS shows that the absorption band in the 200 ~ 350 nm is the charge transfer transition of tungstate group. The luminescent lifetime and quantum efficiency of Ca_2MgWO_6: Eu^{3+} are 0.419 ms and14.05 %, respectively.

Acknowledgments

We are grateful to the support of the Developing Science Fund of Tongji University and the National Natural Science Foundation of China (20671072).

References

[1] A. W. Sleight, R. Ward, J. Am. Chem. Soc. **83**, 1088 (1961).
[2] G. Blasse, A. F. Corsmit, J. Solid State Chem. **6**, 513 (1973).
[3] J. H. G. Bode, A. B. Van Oosterhout, J. Lumin. **10,** 237 (1975).
[4] S. J. Patwe, S. N. Achary, M. D. Mathews, A. K. Tyagi. Mater. Chem. Phys. **98,** 486 (2006).
[5] S. N. Achary, K. R. Chakraborty, S. J. Patwe, A.B. Shinde, P. S. R. Krishna, A. K. Tyagi. Mater Res. Bull **41**, 674 (2006).
[6] S. J. Patwe, S. N. Achary, M. D. Mathews, A. K. Tyagi. J. Alloys Compd. **390**, 100 (2005).
[7] D. F. Li, J. Zheng, Z. G. Zou. J. Phys Chem. Solids **67**, 801 (2006).
[8] C. M. Bonilla, D. A. Landínez Téllez, J. A. Rodríguez, E. Vera López, J. Roa-Rojas. Phys B **398,** 208 (2007).
[9] Goodenough, J. B. Rep. Prog. Phys., **67**, 1915 (2004).
[10] Rylan J. Lundgren, Lachlan M. D. Cranswick, Mario Bieringer. Chem. Mater. **19**, 3945 (2007).
[11] Q. D. Zhou, Brendan J. Kennedy, Margaret M. Elcombe. J. Solid State Chem. **180**, 541 (2007).
[12] Y. Pan, Q. Su, H. Xu, T. Chen, W. Ge, C. Yang, M. Wu, J. Solid State Chem. **174**, 69 (2003).
[13] J. G. Wang, X. P. Jing, C. H. Yan. J. Lumin. **121**, 57 (2006).
[14] B. Grobelna, B. Lipowska, A. M. Klonkowski. J. Alloys Compd. **419,** 191 (2006).
[15] J. Hanuza, M. Maczka, J. H. Van der Maas. J. Solid State Chem. **117**, 177 (1995).
[16] G. Blasse, A. Bril, Z. Phys. Chem. N. F. **57**, 187 (1968)
[17] Q. D. Zhou, B. J. Kennedy, J. H. Christopher, M. E. Margaret, J. S. Andrew, Chem. Mater. **17**, 5357 (2005).
[18] L. D. Carlos, M. A. Bernuy-Lopez, A. B. Craig, B. C. John, J. R. Matthew, Chem. Mater. **19**, 1035 (2007).
[19] R. Mani, P. Selvamani, J. E. Joy, J. Gopalakrishnan. J. Inorg. Chem., **46**, 6661 (2007).
[20] J. Cheng, Z. Q. Yang, Phys. Stat. Sol. (b) **243**, 1151 (2006).
[21] M. Gateshki, J. M. Igartua, A. Faik. J. Solid State Chem. **180**, 2248 (2007).
[22] K. Yamamura, M. Wakeshima, Y. Hinatsu. J. Solid State Chem. **179**, 605 (2006).
[23] T. K. Mandal, J. Gopalakrishnan. Chem. Mater. **17**, 2310 (2005).
[24] M. C. Viola, M. J. Martínez-Lope, J. A. Alonso, J. L. Martínez, J. M. De Paoli, S. Pagola, J. C. Pedregosa, M. T. Fernández-Díaz, R. E. Carbonio. Chem. Mater. **15**, 1655 (2003).
[25] Y. Fujioka, J. Frantti, M. Kakihana. J. Phys. Chem. B **108**, 17012 (2004).
[26] B. Yan, X. Q. Su, Mater. Sci. Eng. B. **116**, 196 (2005).
[27] O. L. Malta, M. A. Couto dos Santos, L. C. Thompson, N. K. Ito, J. Lumin. **69**, 77 (1996).
[28] O. L. Malta, H. F.Brito, J. F. S. Menezes, F. R. Gonc¸alves e Silva, Alves, F. S. Farias, A. V. M. Andrade, J. Lumin., **75**, 255 (1997).
[29] L. D. Carlos, Y. Messaddeq, H. F. Brito, R. A. Sa´ Ferreira, V. deZea Bermudez, S. J. L. Ribeiro, Adv. Mater. **12**, 594 (2000).
[30] R. A. Sa´ Ferreira, L. D. Carlos, R. R. Gonc¸alves, S. J. L. Ribeiro, V. de Zea Bermudez, Chem. Mater. **13**, 2991 (2001).
[31] P. C. R. Soares-Santos, H. I. S. Nogueira, V. Fe´lix, M. G. B. Drew, R. A. Sa´ Ferreira, L. D. Carlos, T. Trindade, Chem. Mater. **15**, 100 (2003).
[32] E. E. S. Teotonio, J. G. P. Espý´nola, H. F. Brito, O. L. Malta, S. F. Oliveria, D. L. A. de Foria, C. M. S. Izumi, Polyhedron **21**, 1837 (2002).
[33] S. J. L. Ribeiro, K. Dahmouche, C. A. Ribeiro, C. V. Santilli, S. H. J. Pulcinelli, J. Sol-Gel Sci. Technol. **13,** 427 (1998).
[34] M. H. V. Werts, R. T. F. Jukes, J. W. Verhoeven, Phys. Chem. Chem. Phys. **4**, 1542 (2002).
[35] C. Y. Peng, H. J. Zhang, J. B. Yu, Q. G. Meng, L. S. Fu, H. R. Li, L. N. Sun, X. M. Guo, J. Phys. Chem. B **109**, 15278 (2005).

*Corresponding author: byan@tongji.edu.cn